Oncogene (2007) 26, 368–381

www.nature.com/onc

ORIGINAL ARTICLE

A soluble ectodomain of LRIG1 inhibits cancer cell growth by attenuating basal and ligand-dependent EGFR activity

S Goldoni[1], RA Iozzo[1], P Kay[1], S Campbell[1], A McQuillan[1], C Agnew[1], J-X Zhu[1], DR Keene[2], CC Reed[1] and RV Iozzo[1,3]

[1]*Department of Pathology, Anatomy and Cell Biology, Thomas Jefferson University, Philadelphia, PA, USA;* [2]*The Shriners Hospital for Children, Portland, OR, USA and* [3]*The Cellular Biology and Signaling Program, Kimmel Cancer Center, Thomas Jefferson University, Philadelphia, PA, USA*

Leucine-rich repeats and immunoglobulin-like domains-1 (LRIG1) is a transmembrane protein with an ectodomain containing 15 leucine-rich repeats (LRRs) homologous to mammalian decorin and the *Drosophila kekkon1* gene. In this study, we demonstrate that a soluble ectodomain of LRIG1, containing only the LRRs, inhibits ligand-independent epidermal growth factor receptor (EGFR) activation and causes growth inhibition of A431, HeLa and MDA-468 carcinoma cells. In contrast, cells that do not express detectable levels of EGFR fail to respond to soluble LRIG1. However, when a functional EGFR gene is introduced in these cells, they become growth-inhibited by soluble LRIG1 protein. Furthermore, we demonstrate the existence of high-affinity ($K_d = 10$ nM) binding sites on the A431 cells that can be competitively displaced (up to 75%) by molar excess of EGF. Even more powerful effects are obtained with a chimeric proteoglycan harboring the N-terminus of decorin, substituted with a single glycosaminoglycan chain, fused to the LRIG1 ectodomain. Both proteins also inhibit ligand-dependent activation of the EGFR and extracellular signal-regulated protein kinase 1/2 signaling in a rapid and dose-dependent manner. These results suggest a novel mechanism of action evoked by a soluble ectodomain of LRIG1 protein that could modulate EGFR signaling and its growth-promoting activity. Attenuation of EGFR activity without physical downregulation of the receptor could represent a novel therapeutic approach toward malignancies in which EGFR plays a primary role in tumor growth and survival.
Oncogene (2007) **26,** 368–381. doi:10.1038/sj.onc.1209803; published online 17 July 2006

Keywords: leucine-rich protein; decorin; kekkon1; epidermal growth factor receptor; tumor growth inhibition

Correspondence: Professor RV Iozzo, Department of Pathology, Anatomy and Cell Biology, Room 249 Jefferson Alumni Hall, Thomas Jefferson University, 1020 Locust Street, Philadelphia, PA 19107, USA.
E-mail: iozzo@mail.jci.tju.edu
Received 28 January 2006; revised 5 June 2006; accepted 5 June 2006; published online 17 July 2006

Introduction

The epidermal growth factor receptor (EGFR) plays a critical role in normal embryonic development and, as a mediator of cell proliferation, it can also drive the growth of tumors through ligand or receptor overexpression or as a receptor gain-of-function mutation (Carpenter, 2000; Carraway and Sweeney, 2001). During evolution, a number of positive and negative regulatory mechanisms for the EGFR signaling have been developed (Moghal and Sternberg, 1999; Schlessinger, 2003). One such mechanism is provided by members of the Kekkon family of transmembrane proteins. The founding member of this family, Kek1, was originally isolated during a screen for genes expressed in *Drosophila* central nervous system (Musacchio and Perrimon, 1996) and was subsequently shown to inhibit EGFR activity during oogenesis (Ghiglione *et al*., 1999), as well as in the developing eye and wing (Alvarado *et al*., 2004a, b; Ghiglione *et al*., 2003). In *Drosophila*, Kek1 is a transcriptional target of the EGFR where it attenuates receptor activity through an inhibitory feedback loop (Ghiglione *et al*., 1999). Kek1 is one of six Kekkon family members, all of which share a similar architecture: seven leucine-rich repeats (LRR) capped by two Cys-rich flanking domains, a single Ig domain, a transmembrane domain and a cytoplasmic tail. Kek1 is the only member that inhibits EGFR activity (Alvarado *et al*., 2004a) as shown by the discovery of two finite classes of disrupted *Kek1* alleles (Alvarado *et al*., 2004b). Class I mutant alleles have mutations in the LRRs, whereas class II alleles have mutations in the flanking Cys-rich and immunoglobulin (Ig) domains. These mutant alleles are not only physically but also functionally distinct. Class I alleles reduce Kek1 affinity for the EGFR, whereas class II alleles disrupt Kek1 subcellular localization, thereby altering Kek1 ability to interact with the EGFR (Alvarado *et al*., 2004b). *Kek1* is highly conserved across species during evolution. In fact, orthologs of *Kek1* are found in three Dipteran species, suggesting that Kek1 ability to suppress EGFR activity was present over 40–65 million years ago (Derheimer *et al*., 2004). Ectopic expression of Kek1 in mammalian cells leads to an interaction with all the four members of the ErbB

family of receptor tyrosine kinase, and to a suppression of growth factor binding and receptor activation (Ghiglione *et al*., 2003). Kekkon members are absent in vertebrates and the invertebrate *Caenorhabditis elegans*. However, these species express a family of transmembrane proteins containing both LRRs and Ig domains, called LIG (Suzuki *et al*., 1996; Carraway and Sweeney, 2001; Nilsson *et al*., 2001; Suzuki *et al*., 2002) or LRIG (Nilsson *et al*., 2003; Guo *et al*., 2004; Holmlund *et al*., 2004), considered to be distant family relatives.

The mammalian LRIG1 protein contains 15 LRRs, three Ig repeats, a transmembrane domain and a cytoplasmic tail. *LRIG1* is located on chromosome 3p14 (Nilsson *et al*., 2001), a region frequently deleted in various human cancers, consistent with reduced or absent expression in renal cell carcinomas and various transformed cell lines (Hedman *et al*., 2002; Thomasson *et al*., 2003). Notably, mice deficient in *Lrig1* show a psoriasis-like epidermal hyperplasia (Suzuki *et al*., 2002), with a phenotype resembling that observed in transgenic mice over-expressing the two EGFR ligands tumor growth factor (TGF)-α and amphiregulin, in the stratified squamous epithelia (Cook *et al*., 1997; Vassar and Fuchs, 1991). Consistent with a role in attenuating EGFR signaling, expression of the transmembrane LRIG1 promotes receptor ubiquitination and degradation (Gur *et al*., 2004; Laederich *et al*., 2004).

We have previously shown that decorin, a secreted small leucine-rich proteoglycan (Iozzo, 1999), is capable of directly interacting with the EGFR (Iozzo *et al*., 1999; Santra *et al*., 2002) and downregulating its activity both *in vitro* and *in vivo* (Csordás *et al*., 2000; Reed *et al*., 2002; Reed *et al*., 2005). Thus, we hypothesized that a soluble form of LRIG1 could similarly affect the EGFR signaling pathway. In this study, we demonstrate that the ectodomain of LRIG1 (LRIG1^{ecto}), containing only the LRRs and flanking Cys-rich caps, inhibits both ligand-dependent and ligand-independent EGFR activation and extracellular signal-regulated protein kinase1/2 (Erk1/2) signaling in a dose-dependent manner, and causes growth inhibition of A431, HeLa and MDA-468 carcinoma cells. In contrast, cells that do not express detectable levels of EGFR fail to respond to soluble LRIG1. We demonstrate the existence of high-affinity ($K_d = 10$ nM) binding sites on the A431 cells, and the vast majority of these (up to 75%) can be competitively displaced by EGF. A chimeric proteoglycan harboring the N-terminal part of decorin, substituted with a single glycosaminoglycan chain, fused to the LRIG1 ectodomain (Dcn-LRIG1^{ecto}), shows even more powerful effects. These results suggest that the soluble ectodomain of LRIG1 could act as a negative regulator of the EGFR signaling pathways.

Results

Alignment of LRRs of LRIG1, decorin and Kek1

The mammalian LRIG1 protein contains 15 LRRs, three Ig repeats, a transmembrane domain and a cytoplasmic tail. As decorin contains only LRRs and yet has a biological activity similar to that of Kek1 and LRIG1, we studied in detail the LRR regions in LRIG1, decorin and Kek1, with the premise that the LRR domain is the actual interacting domain between these molecules and the EGFR. The LRRs of these three molecules aligned quite well (Figure 1a). Alignment of the abutting Cys-rich regions of all three molecules revealed a close homology of the three, especially in the N-terminal Cys-rich region (Figure 1b). However, our analysis revealed a most interesting relationship among the three proteins: both decorin and Kek1 align nearly identically over a central portion of LRIG1's repeats, with the exception of LRIG1 LRR_{8-9}, where a conserved deletion in both decorin and Kek1 exists relative to LRIG1 (Figure 1c). The deletion removes one-half of LRR_8 and one-half of LRR_9, resulting in the relative loss of one complete LRR in decorin and Kek1 as compared to LRIG1. The primary region of decorin shown to interact with EGFR is LRR_6 (Santra *et al*., 2002), which corresponds to LRR_{10} of LRIG1 and to LRR_3 of Kek1, respectively. Conceivably this region could be important in a putative LRIG1–EGFR interaction. This is remarkable, because a recent study has identified that mutations in the LRR_{2-3} of Kek1 cause a reduced affinity for the EGFR (Alvarado *et al*., 2004b). Especially important is Gly^{160} in Kek1's LRR_2, suggesting that this residue has a crucial role in directing Kek1 interaction with the EGFR. Two of these mutant alleles encode a change to Ser (G160S), whereas a third mutant allele of Kek1 encodes a conversion to Asp (G160D); all these mutants result in complete suppression of Kek1 activity (Alvarado *et al*., 2004b). On the basis of these results, we predict that a similar region in LRIG1 would be involved in EGFR binding, in analogy to decorin and Kek1.

Expression and characterization of human recombinant LRIG1^{ecto} and Dcn-LRIG1^{ecto}

To investigate the role of soluble LRIG1, we generated two truncated variants of LRIG1: one containing the 15 LRRs and a chimera containing the LRRs fused to the first 24 amino-acid residues of human decorin (Figure 1d). The latter contains the Ser-Gly sequence responsible for substitution with a single glycosaminoglycan chondroitin/dermatan side chain (Iozzo, 1998). The recombinant LRIG1^{ecto} generated in 293-EBNA cells migrated as a single band of $\sim$65 kDa, consistent with a glycosylated protein (the predicted size from the sequence is $\sim$51 kDa). In contrast, Dcn-LRIG1^{ecto} migrated primarily as a broadband centering at $\sim$120 kDa, typical of proteoglycan migration in sodium dodecyl sulfate–polyacrylamide gel electrophoresis (SDS–PAGE), in addition to unglycanated protein core migrating at $\sim$65 kDa as the parent LRIG1^{ecto} (Figure 1e). Condroitinase ABC digestion, which cleaves both chondroitin and dermatan sulfate, converted the Dcn-LRIG1^{ecto} into the protein core (Figure 1f), indicating that Dcn-LRIG1^{ecto} was substituted with a chondroitin/dermatan sulfate chain as decorin.

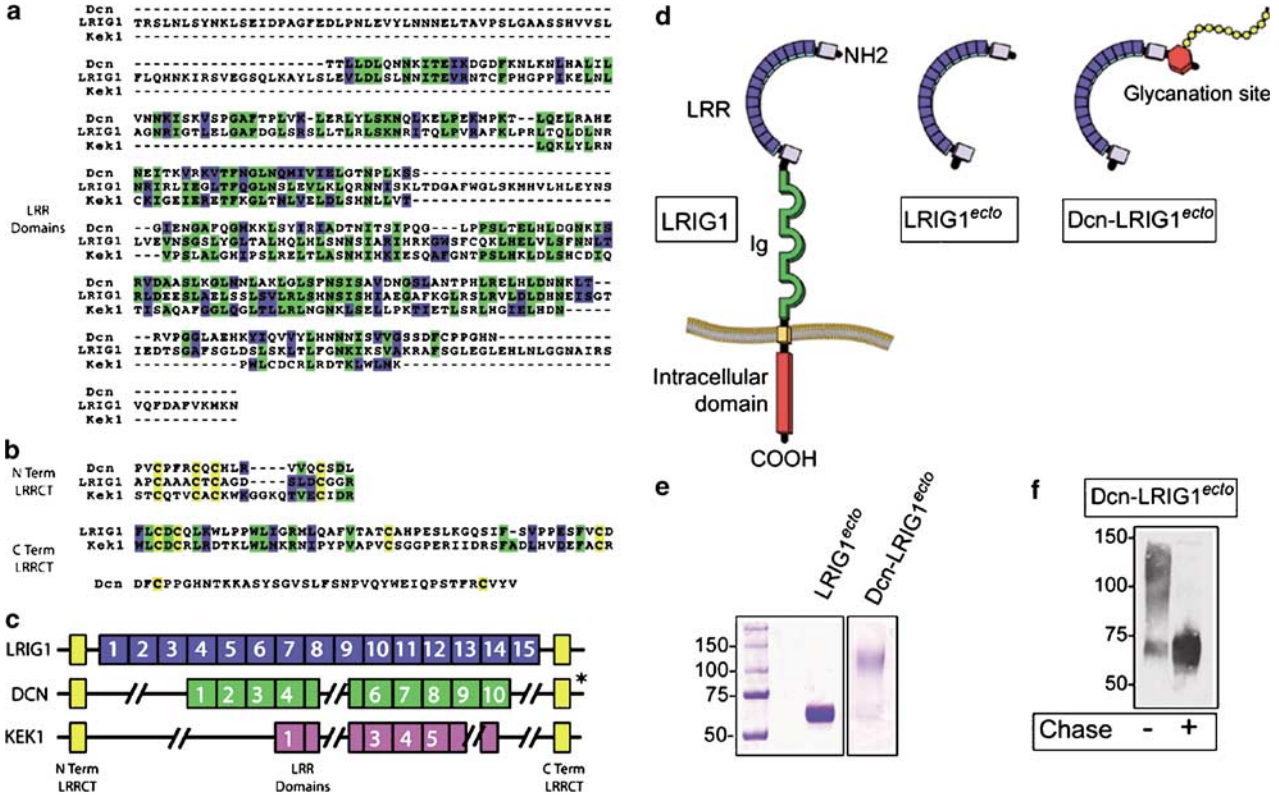

Figure 1 Sequence alignments of LRIG1, decorin and the *Drosophila* Kekkon1, and characterization of LRIG1 soluble ectodomain. (**a**) Multiple sequence alignment of the LRRs of LRIG1, decorin and Kek1 performed with CLUSTALW and colored with BOXSHADE. Both algorithms were implemented in Biology Workbench (workbench.sdsc.edu). Identical residues are green, and conserved residues are blue. (**b**) Alignments of the cysteine-rich regions that cap the LRRs of LRIG1, decorin and Kek1. The residue color scheme is identical to (**a**), with the exception of conserved cysteine residues, which are colored yellow. The locations of cysteine residues at the N-terminal region in both decorin and LRIG1 match the canonical CX_3CXCX_6C pattern of class I SLRPs (Iozzo and Murdoch, 1996; Iozzo, 1997). The Cys-rich region of Kek1 contains a gap of 10 residues before the final cysteine, more reminiscent of class II SLRPs that by definition have a gap of nine residues. The C-terminal Cys-rich region of LRIG1 and Kek1 contains a conserved LRR protein C-terminal region ($CXCX_{21}CX_{20-21}C$) as identified by the NCBI Conserved Domain Database (www.ncbi.nlm.nih.gov). The C terminus of decorin, while also Cys-rich, contains a different pattern of residues. (**c**) Schematic representation showing the modular nature of conserved domains of LRIG1, decorin and Kek1. Cys-rich domains are colored yellow, and well-conserved LRRs are numbered. Gaps in the alignment are indicated by //. (**d**) Schematic representation of the full-length LRIG1, LRIG1^{ecto} and Dcn-LRIG1^{ecto} chimeric proteoglycan as indicated. (**e**) Coomassie-stained acrylamide gel of purified proteins as indicated. The first lane includes standard proteins. Note that Dcn-LRIG1^{ecto} is composed primarily by the proteoglycan form with a relatively small fraction of non-glycanated protein core. (**f**) Immunoblotting of Dcn-LRIG1^{ecto} (~200 ng) before and after chondroitinase ABC (Chase) digestion using an anti-His antibody. Note that the chimeric proteoglycan is converted to the protein core following removal of the chondroitin/dermatan sulfate side chain.

Next, we determined the appearance of the soluble LRIG1 ectodomain by rotary shadowing electron microscopy. Nearly all the images of isolated LRIG1^{ecto} and Dcn-LRIG1^{ecto} showed an arch-shaped structure (Figure 2a), slightly larger and more extended than that observed with the decorin protein core (Keene *et al*., 2000). Quantitative analysis of 300 LRIG1^{ecto} molecules (Figure 2b) gave an average size of 14.8 ± 1.4 nm (the distance between the two arms) by 10.5 ± 1.4 nm (the distance between the base of the arch and the apex). Analysis of 150 Dcn-LRIG1^{ecto} molecules showed them to be of similar but not identical size to LRIG1^{ecto}, with dimensions of 15.8 ± 1.9 by 11 ± 1.6 nm.

LRIG1^{ecto} *and Dcn-LRIG1*^{ecto} *selectively inhibit the growth of EGFR-expressing cells*

To determine whether soluble recombinant LRIG1^{ecto} and Dcn-LRIG1^{ecto} would influence cell growth in a paracrine manner and to mimic a more physiological situation, we established a co-culture system where 293-EBNA cells, either wild-type or stably expressing cells, were seeded in the top wells of trans-well dishes, whereas A431 cells were seeded in the bottom wells. Under such conditions, only soluble factors released from the cells would be able to diffuse through the 0.2-μm membrane separating the two compartments. Notably, both LRIG1^{ecto} and Dcn-LRIG1^{ecto} markedly inhibited the growth of A431 squamous carcinoma cells in the presence of full serum (Figure 3a). At 6 days of co-culture, the growth of A431 cells was inhibited by ~55 and ~68% when co-cultured with LRIG1^{ecto}-or Dcn-LRIG1^{ecto}-secreting cells, respectively ($P < 0.01$). To eliminate the possibility that the growth-inhibitory activity was caused by an unknown activity present in the clonal cells, we transfected 293-EBNA cells with the empty pCEP-Pu vector and compared the effects to those obtained by LRIG1-secreting cells using

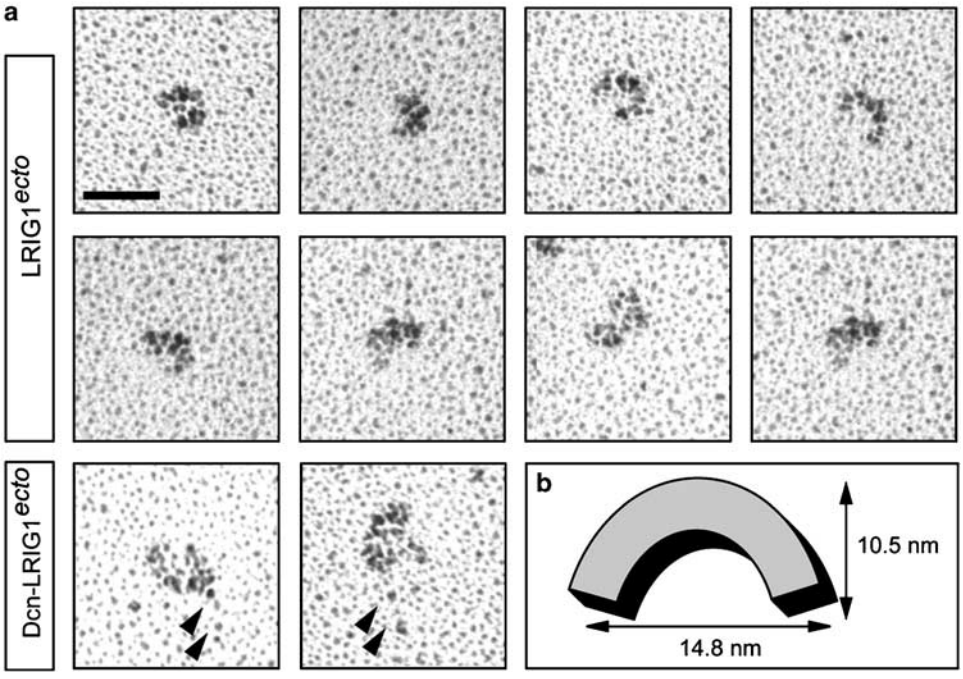

Figure 2 Rotary shadowing electron microscopy of isolated LRIG1^{ecto} and Dcn-LRIG1^{ecto}. (**a**) Size analysis of LRIG1^{ecto} and Dcn-LRIG1^{ecto} molecules from rotary-shadowed images were inspected and measured using the public domain NIH Image program (http://rsb.info.nih.gov/nih-image/). Rotary-shadowed images of LRIG1^{ecto} molecules revealed a concave molecule, similar in structure to known LRR protein structures. The two final panels show a similar structure for Dcn-LRIG1^{ecto}, as well as possible glycosaminoglycan chains, indicated by arrowheads. Scale bar = 20 nm. (**b**) Diagram of LRIG1^{ecto} based on rotary-shadowed measurements. Analysis of 300 LRIG1^{ecto} molecules gave a mean size of 14.8 ± 1.4 nm by 10.5 ± 1.4 nm. Analysis of 150 Dcn-LRIG1^{ecto} molecules gave dimensions of 15.8 ± 1.9 nm by 11.0 ± 1.6 nm.

co-culture experiments as described above. The results showed that after 4 days of co-culture, there was ~45% inhibition of growth caused by the LRIG1 ectodomain-secreting cells ($P < 0.05$, Figure 3b).

To establish more directly that the growth inhibitory effects were owing to the presence of the recombinant proteins, rather than to the physical presence of the 293-EBNA cells, we performed growth assays using either conditioned medium (5× concentrated by ultrafiltration) or purified recombinant proteins. The concentrated conditioned media containing either recombinant protein markedly (>70%) suppressed the growth of HeLa and A431 (Figure 3c). Similar results were obtained with recombinant LRIG1^{ecto} (0.45 μM) (Figure 3d). Notably, both A431 cells, which contain $\sim 2.5 \times 10^6$ EGFR per cell (Csordás *et al*., 2000), and HeLa cells, which contain $\sim 5 \times 10^4$ receptors per cell (Berkers *et al*., 1991; Sigismund *et al*., 2005), equally responded to the growth inhibitory activity evoked by LRIG1^{ecto} and Dcn-LRIG1^{ecto}. As in the case of the co-culture, the media from empty vector-transfected cells had no significant effect on the growth of either A431 or HeLa cells (Figure 3c). Moreover, we performed a growth inhibition assay using an A431 clone recently produced in our laboratory by long-term treatment with EGF (Zhu *et al*., 2005). Although these cells express ~40% of the EGFR levels expressed by wild-type cells, they were similarly growth inhibited by both the ectodomain of LRIG1 and Dcn-LRIG1 (not shown). These findings suggest that the biological activity of these two proteins does not depend on receptor density.

The growth-suppressive activity of both LRIG1^{ecto} and Dcn-LRIG1^{ecto} was further assessed in MDA-468 breast carcinoma cells, which have an amplified EGFR and express $\sim 1.9 \times 10^6$ receptors per cell (Filmus *et al*., 1985, 1987; Ennis *et al*., 1989). In these experiments, the recombinant proteins (0.45 μM) were added every day together with fresh medium containing 10% fetal calf serum. Notably, there was a ~50% inhibition by LRIG1^{ecto} and >90% inhibition by Dcn-LRIG1^{ecto} (Figure 3e). These findings suggest that the soluble LRRs of LRIG1 and especially the chimeric proteoglycan can affect the growth of a variety of transformed cell lines that express EGFR.

EGFR expression is required for the activity of LRIG1 ectodomain

To further investigate whether EGFR expression was required for LRIG1-mediated cytostatic effects, we utilized CHO-K1 cells, which do not express EGFR (Figure 4a). We found that CHO-K1 cells, in contrast to A431 cells, did not respond to the medium containing either LRIG1^{ecto} or Dcn-LRIG1^{ecto} (Figure 4b). Similar results were obtained when cells were exposed to recombinant LRIG1 ectodomain (not shown). Next, we tested whether CHO-K1 cells with *de novo* expression of EGFR would respond to LRIG1^{ecto}. To this end, we

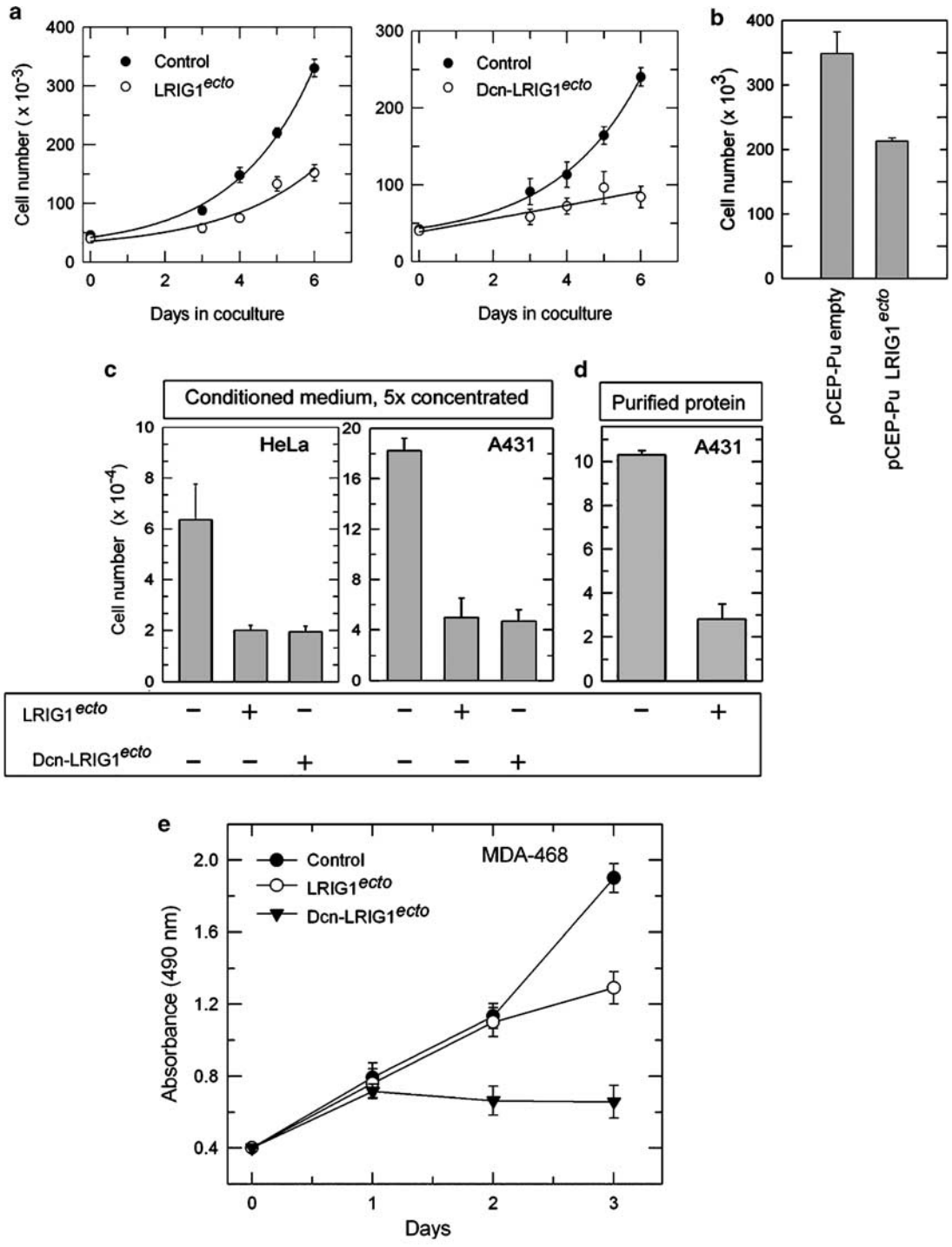

Figure 3 LRIG1^{ecto} and Dcn-LRIG1^{ecto} suppress the growth of several carcinoma cells. (**a**) Co-culture of wild-type 293 cells (•) or LRIG1^{ecto}- and Dcn-LRIG1^{ecto}-secreting 293 cells (○) with A431 cells. Equal numbers of target cells (A431) were plated in the bottom chamber of a transwell apparatus, whereas the secreting cells were placed in the top chambers separated by a 0.2-μm filter. The values represent the mean $\pm$ s.e.m. of three independent experiments; each measurement was performed in triplicate. (**b**) Effects of co-culturing (4 days) A431 cells in the presence of 293-EBNA cells transfected with either empty or LRIG1^{ecto}-containing pCEP-Pu vector. The values represent the mean $\pm$ s.e.m. of a triplicate experiment. (**c**) Effects of concentrated media containing recombinant LRIG1^{ecto} or Dcn-LRIG1^{ecto} proteins. Controls were incubated with conditioned medium from 293-EBNA cells transfected with empty pCEP-Pu vector. (**d**) Effects of recombinant LRIG1^{ecto} on A431 cell growth (0.45 μM, for 48 h). (**e**) Time-course effects of recombinant LRIG1^{ecto} (○), Dcn-LRIG1^{ecto} (▼) or vehicle control (•) on the growth of MDA-468 breast carcinoma cells. In these experiments, recombinant proteins (0.45 μM) were freshly added every day together with serum-containing media. Cell number was estimated by determining OD at 490 nm using the CellTiter 96 assay (Promega). The values represent the mean $\pm$ s.e.m. of three measurements.

transfected wild-type CHO-K1 cells with a vector containing the whole EGFR linked to the cyan fluorescent protein (CFP) at its C-terminus. It has been previously shown that this EGFR, carrying either a GFP or a CFP, is fully viable and signals in response to EGF, and has been successfully used to study EGFR endocytosis, trafficking and interaction with various adaptor proteins (Carter and Sorkin, 1998; Sorkin *et al*., 2000; Jiang and Sorkin, 2002; Jiang *et al*., 2003) and chemotactic responses (Bailly *et al*., 2000). Immunoblotting of total cell lysates showed the expression of a ~200-kDa EGFR-CFP chimera in the CHO-K1 11A3 cells (Figure 4c). As positive control, we used A431 cell extracts, which showed the ~175 kDa EGFR. From the immunoblotting, we estimated that the CHO-K1 11A3 cells contained about 15% of the total EGFR expressed by A431 or $\sim 3.4 \times 10^5$ EGFR/cell. Immunoblotting with PY20 demonstrated rapid Tyr phosphorylation of the EGFR-CFP and a number of cellular proteins upon stimulation with EGF (Figure 4d), in agreement with published reports (Carter and Sorkin, 1998; Sorkin *et al*., 2000). Fluorescence microscopy of CHO-K1 11A3 cells showed a strong endogenous EGFR-CFP signal at the cell surface (Figure 4e), which colocalized with

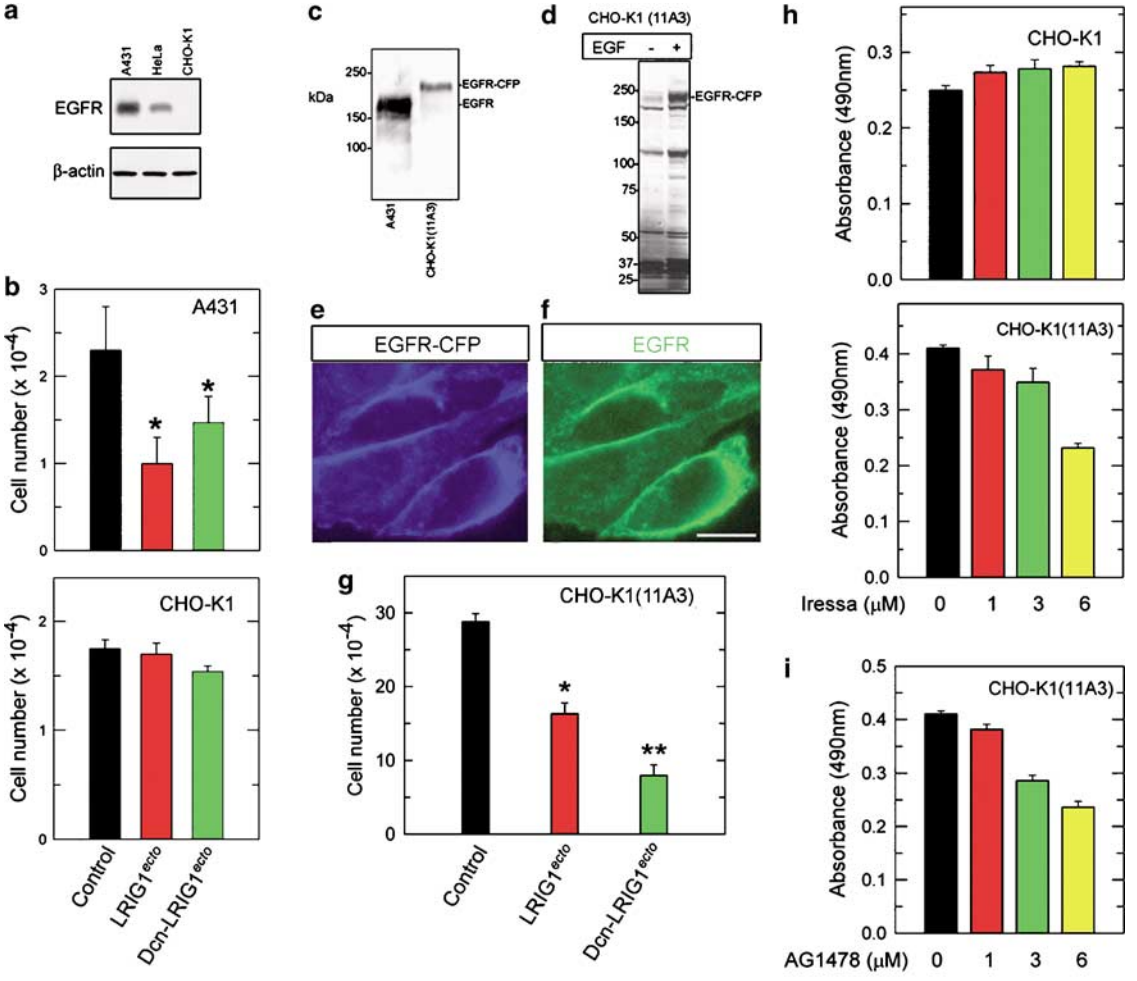

Figure 4 EGFR requirement for LRIG1^{ecto}-mediated inhibition of cell growth. (**a**) Western immunoblotting of total cell lysates using an antibody against either the EGFR or β-actin. Note the lack of any detectable EGFR in the CHO-K1 cells. (**b**) Growth assay of A431 or CHO-K1 cells following a 3-day exposure to 5× concentrated conditioned media containing either LRIG1^{ecto} or Dcn-LRIG1^{ecto} as indicated. Similar results were obtained when cells were exposed to recombinant LRIG1 ectodomains (not shown). The values are the mean ± s.e.m. of three measurements ($P<0.05$). (**c**) Immunoblotting of total cell lysates using an anti-EGFR antibody. Notice the presence of a ~200-kDa EGFR-CFP in the clone 11A3. (**d**) Immunoblotting with PY20 demonstrates rapid Tyr phosphorylation of the EGFR-CFP and a number of cellular proteins upon stimulation with EGF (16 nM, 30 min). (**e**) Fluorescence microscopy of clone 11A3 showing endogenous EGFR-CFP with a strong cell surface signal. The image was captured using a cyan filter (Olympus). (**f**) Immunofluorescence microscopy of the same cells using an anti-EGFR antibody and a FITC-labeled secondary antibody. Notice the near complete overlap of the two signals. Scale bar = 5 μm. (**g**) Growth assay of the CHO-K1 cells expressing the EGFR-CFP following a 2-day exposure to recombinant LRIG1^{ecto} or Dcn-LRIG1^{ecto} (0.45 μM) as indicated. The values are the mean ± s.e.m. of three measurements (*$P<0.05$, **$P<0.01$). (**h**) Growth assay of CHO-K1 and CHO-K1 EGFR-CFP-expressing cells (11A3) following a 4-day treatment with increasing concentration of Iressa, as indicated, in medium containing serum. (**i**) Growth inhibition of CHO-K1 (11A3) cells following a 4-day treatment with AG1478, in medium containing serum. Control wild-type cells behaved as in panel h and they are not shown. Values were obtained by determining OD at 490 nm using the CellTiter96 assay (Promega) and represent the mean ± s.e.m. of three measurements.

EGFR (Figure 4f). When the CHO-K1 11A3 cells were exposed to recombinant LRIG1^{ecto} or Dcn-LRIG1^{ecto} (0.45 μM), there was a significant growth inhibition (Figure 4g). These results are even more striking if we take into consideration that the cells used for these assays are a mixed population derived from mass culture, thereby eliminating the problem with 'clonality'. As in the case of the A431 and HeLa cells, media conditioned by 293-EBNA transfected with an empty pCEP-Pu vector had no appreciable effect on the growth of CHO-K1 or CHO-K1 11A3 cells (not shown).

To further prove specificity (i.e., determine if EGFR-transfected cells became dependent on EGFR signaling for their growth), we utilized two different EGFR-specific tyrosine kinase inhibitors, gefitinib (Iressa) (Sordella *et al*., 2004; Pao and Miller, 2005) and the tyrphostin AG1478 (Levitzki and Gazit, 1995). In contrast to the wild-type CHO-K1 cells, the EGFR-expressing CHO-K1 cells were inhibited by both kinase inhibitors in a concentration-dependent manner (Figure 4h and i).

Collectively, these results provide strong genetic evidence for the EGFR requirement in LRIG1-evoked activity and further validate the results presented in the previous sections.

Soluble LRIG1 ectodomain specifically interacts with the EGFR

Having established the EGFR requirement for LRIG1^{ecto}-mediated activity, we next determined whether a direct and specific interaction between the receptor and the soluble ligand did indeed occur with live cells. To this end, we radioiodinated recombinant LRIG1^{ecto} with ^{125}I and Iodogen beads (Pierce, Rockford, IL, USA) to reach high specific activity ($1–8 \times 10^{18}$ c.p.m./mol) and purified it via a Sephadex G-50 column. The eluted fractions (fraction nos. 12–15, Figure 5a) gave a single peak, which was shown by SDS–PAGE and autoradiography to be pure LRIG1^{ecto} (Figure 5b). Radioligand binding studies using confluent A431 cells at 4°C showed saturable binding (Figure 5c) with a K_d of 10 ± 1.2 nM (Figure 5d). Specificity of the binding was further proven by competitive displacement of radiolabeled LRIG1^{ecto} by 10- and 20-fold molar excess of cold EGF (Figure 5e; $P < 0.01$).

Next, we performed overlay assays using increasing amounts of either BSA or LRIG1^{ecto} immobilized on nitrocellulose filter and then incubated with serum-free medium conditioned by A431 cells. The latter contains a soluble form of EGFR, which lacks the transmembrane and intracytoplasmic domain (Weber *et al*., 1984; Yarden *et al*., 1985). This soluble protein (Figure 5f, top left) is derived from a 2.8 kb mRNA transcribed from a rearranged *EGFR* gene on chromosome 7 (Carpenter, 1987). The results showed that the soluble EGFR specifically and dose dependently bound to immobilized LRIG1^{ecto}, in contrast to BSA that was unreactive. This is important because the slot-blot overlay assay utilizes non-denaturing conditions and, thus, it supports a physiological interaction. Also, the

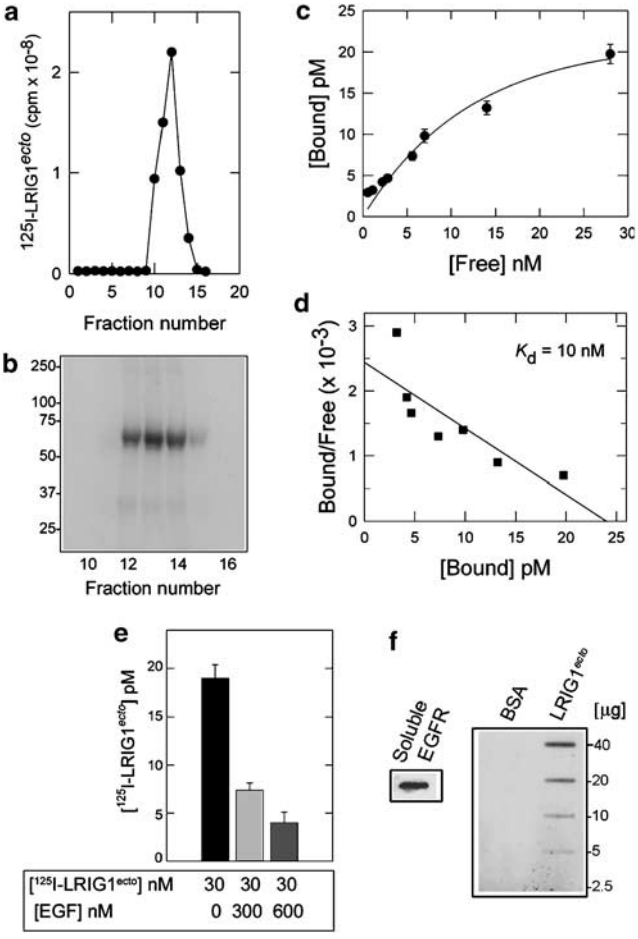

Figure 5 Specific binding between soluble LRIG1 ectodomain and the EGFR. (**a**) Elution profile of radioiodinated LRIG1^{ecto}. (**b**) SDS–PAGE of the elution fractions 11–16. (**c**) Saturation binding curve. Quiescent, serum-starved A431 cells were incubated with increasing concentration of radiolabeled LRIG1^{ecto} at 4°C in M199 medium/0.1% BSA. (**d**) Scatchard plot of the data in panel c. (**e**) Competition experiment using 10- and 20-fold molar excess of cold EGF. $P < 0.01$, $n = 3$. (**f**) Overlay assay using various amounts of either BSA or LRIG1^{ecto}, as indicated. Slot blots were incubated for 16 h with serum-free media conditioned by A431 cells that contain the soluble form of EGFR, as shown in the left panel. The blots were washed extensively and incubated with an anti-EGFR antibody followed by chemiluminescence detection.

^{125}I-labeled LRIG1 specifically bound to immobilized soluble EGFR but not to EGF, using similar overlay assays (not shown). This eliminates the possibility that LRIG1 might interfere with EGFR activity by blocking EGF. These findings provide for the first time a direct and specific interaction between the ectodomain of LRIG1 and the ectodomain of the EGFR where the ligand-binding region is present.

LRIG1^{ecto} and Dcn-LRIG1^{ecto} attenuate ligand-independent and ligand-dependent EGFR signaling

Given the profound growth inhibitory activity of soluble LRIG1, we tested whether this biological property could be owing to interference with basal (ligand-independent) EGFR activity. Serum-starved, quiescent A431 cells

were incubated for ~2 h with increasing concentrations of either protein and the levels of total phospho-tyrosine (P-Tyr), EGFR P-Tyr1068, an established autophosphorylation site of the EGFR intracellular domain, and total EGFR were determined by immunoblotting. The results showed a marked and dose-dependent suppression of EGFR autophosphorylation for both *LRIG1*^{ecto}- and Dcn-*LRIG1*^{ecto}-treated cells (Figure 6a and c), with an IC_{50} of ~2 nM for both proteins (not shown). Time-course experiments using equimolar amounts of either protein showed a time-dependent suppression of basal EGFR activation, with $T_{1/2}$ of ~45 and ~10 min for LRIG1^{ecto} and Dcn-LRIG1^{ecto}, respectively (Figure 6b and d).

Next, we tested whether LRIG1^{ecto} would affect ligand-dependent activation of the EGFR. Pre-incubation of quiescent A431 cells with LRIG1^{ecto} for 1 or 2 h blocked EGF-induced EGFR phosphorylation at Tyr1068 by ~50% (Figure 7a and b), without affecting the endogenous EGFR levels. Similarly, phosphorylation of Erk1/2, an established downstream component of the EGFR signaling pathway, was inhibited by ~35% after 1 h, and by ~75% after 2 h (Figure 7c and d). Comparable results were obtained with Dcn-LRIG1^{ecto} (not shown). Using shorter incubation times (5–30 min), soluble LRIG1 ectodomain did not cause any appreciable activation of the Erk1/2 pathway (not shown).

Next, we carried out a more detailed analysis of LRIG1-dependent attenuation of EGFR signaling by performing a dose–response study. In these experiments, quiescent A431 cells were pre-incubated for 2 h with a constant dose of LRIG1^{ecto} or Dcn-LRIG1^{ecto} (0.45 μM) and in the last 10 min of incubation various concentrations of EGF were added. The results showed a marked inhibition of EGF-induced phosphorylation at Tyr1068 (Figure 7e). Quantification of various experiments showed that at a sub-optimal EGF concentration (10 ng ml^{-1} = 1.6 nM) EGFR activation was blocked by over 90%, while at maximal EGF concentration (16 nM) EGFR activation was blocked by ~65% (Figure 7f). Thus, soluble forms of LRIG1 containing the LRRs are capable of affecting both ligand-dependent and ligand-independent activation of the EGFR, without any appreciable downregulation of the total receptor.

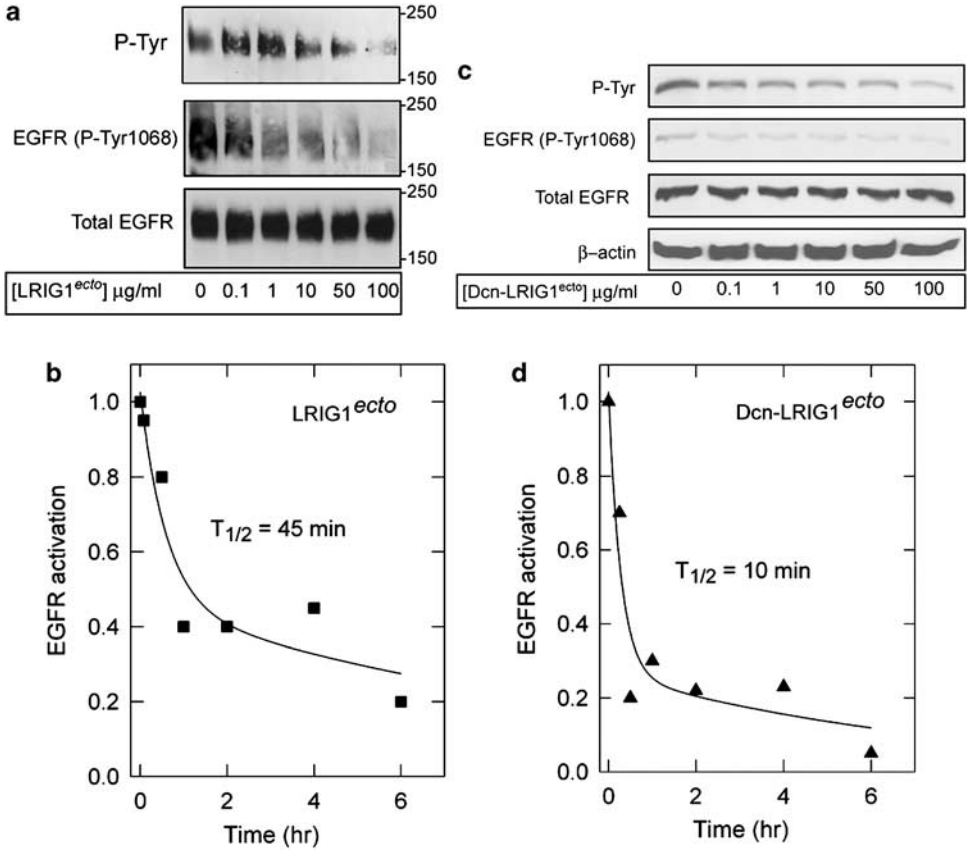

Figure 6 LRIG1^{ecto} and Dcn-LRIG1^{ecto} attenuate ligand-independent EGFR signaling. (**a**, **c**) Western immunoblottings of total A431 cell lysate following treatment with LRIG1^{ecto} or Dcn-LRIG1^{ecto} at the designated concentrations using antibodies against P-Tyr, EGFR phosphorylated at Tyr1068, a common autophosphorylation site, total EGFR and β-actin. (**b**, **d**) Time-course inhibition of EGFR phosphorylation (activation) by LRIG1^{ecto} (■) and Dcn-LRIG1^{ecto} (▲), respectively. The values were obtained from additional blots (not shown) and represent mean ± s.e.m. of three experiments. In these experiments, quiescent A431 cells were exposed to 0.45 μM of each protein and the EGFR activation was measured by immunoblotting as in panel a, followed by scanning densitometry with the NIH Scion Image software.

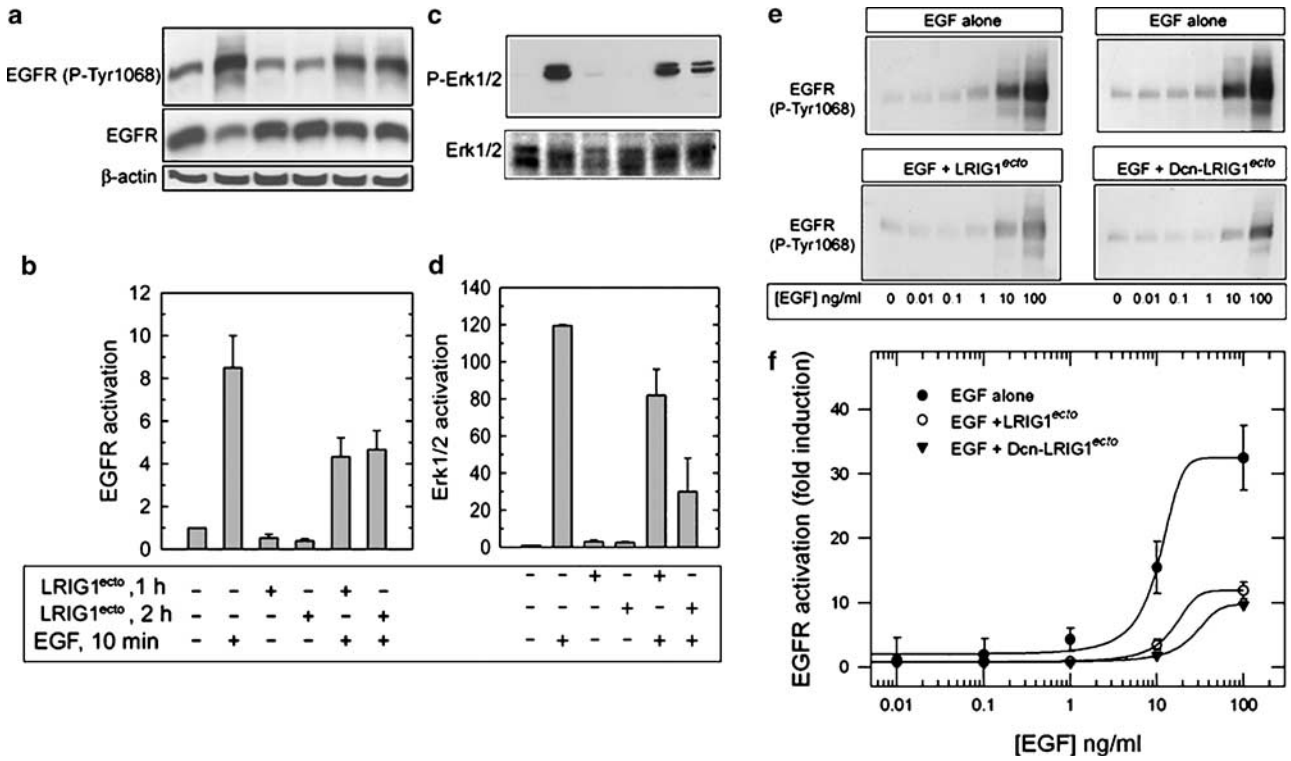

Figure 7 LRIG1^{ecto} and Dcn-LRIG1^{ecto} suppress ligand-dependent activation of the EGFR. (**a**) Immunoblotting of total A431 cell lysates treated for 1 or 2 h with 0.45 μM LRIG1^{ecto}. The immunoblottings were reacted with antibodies against EGFR P-Tyr1068, total EGFR or β-actin. (**b**) Quantification of EGFR P-Tyr1068 shows significant suppression of EGF-dependent EGFR phosphorylation by soluble LRIG1 protein. The values represent the mean$\pm$s.e.m. of three independent experiments. (**c**) Immunoblotting of the bottom part of the gel identical to that shown in panel a. Note the suppression of Erk1/2 phosphorylation, an established downstream component of the EGFR signaling pathway. (**d**) Quantification of Erk1/2 phosphorylation. The values represent the mean$\pm$s.e.m. of three independent experiments. (**e**) Immunoblotting of quiescent A431 cells pre-incubated for 2 h with a constant dose of LRIG1^{ecto} or Dcn-LRIG1^{ecto} (0.45 μM); in the last 10 min of the incubation, various concentrations of EGF were added as indicated. Note the marked inhibition of EGF-induced phosphorylation at Tyr1068. (**f**) Quantification of three independent experiments similar to those shown in panel e. The values are the mean$\pm$s.e.m. Note that at a sub-optimal EGF concentration (1.6 nM) of EGFR activation was blocked by over 90%, whereas at maximal EGF concentration (16 nM) of EGFR activation was blocked by $\sim$65%.

LRIG1 induces neither EGFR internalization nor EGFR phosphorylation at Tyr1045

The data presented so far indicate that soluble forms of LRIG1 ectodomain do not induce a downregulation of the EGFR, as its levels were not significantly affected by these proteins. If this were the case, then, the EGFR should not be diverted into an intracellular degradation pool by soluble LRIG1 protein. To test this hypothesis, we incubated quiescent A431 cells with either recombinant protein for 30 min with or without chase for 90 min in serum-free media. Under quiescent conditions, the EGFR was localized primarily at the cell surface (Figure 8a). Exposure of the cells to EGF evoked a rapid mobilization of the receptor into cytoplasmic vesicles (Figure 8b), in agreement with previous studies (Carter and Sorkin, 1998; Bailly *et al*., 2000; Carpenter, 2000). In contrast, exposure of the cells to either recombinant protein did not cause any appreciable EGFR movement into the cytoplasm (Figure 8c–f). Immunofluorescence microscopy of cells exposed to LRIG1^{ecto} (0.45 μM) for 30 min showed a marked colocalization of both proteins at the cell surface (Figure 8g–i), without any significant internalization of the receptor. In agreement with these findings, recombinant LRIG1 proteins did not cause any substantial phosphorylation of EGFR at Tyr1045, whereas EGF caused up to a 30-fold increase in phosphorylation of this key amino-acid residue (Figure 8j and k). This is important as phosphorylation at Tyr1045 creates a major docking site for c-Cbl, which mediates ligand-induced ubiquitination and downregulation of the receptor (Levkowitz *et al*., 1999; Grovdal *et al*., 2004). In cells expressing EGFR mutated at Tyr1045, c-Cbl retains residual activity by docking to Grb2, thereby leading to the retardation of receptor endocytosis and acceleration of its recycling to the cell surface (Waterman *et al*., 2002). One of the docking sites for Grb2 on the tyrosine kinase domain of the EGFR is Tyr1068 (Batzer *et al*., 1994; Okutani *et al*., 1994). The fact that soluble LRIG1 protein negatively regulates Tyr1068 phosphorylation (see Figures 6 and 7) is in support of LRIG1-mediated inhibition of mitogenic signaling and recycling of the receptor to the cell surface.

Collectively, our results indicate that soluble forms of LRIG1 protein attenuate EGFR activity without any significant internalization or degradation of the receptor, and provide a novel mechanism of action for this class of molecules.

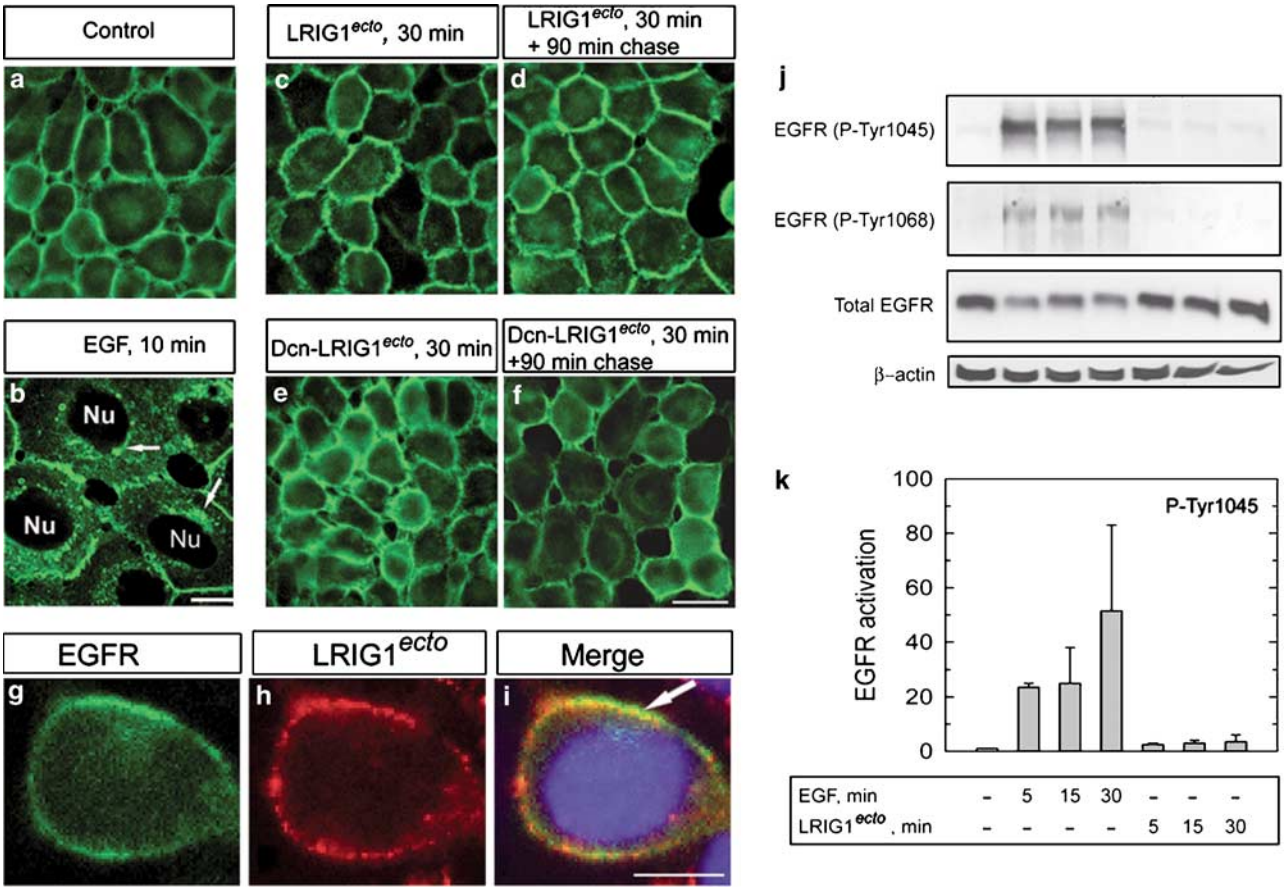

Figure 8 LRIG1^{ecto} does not induce appreciable EGFR internalization or EGFR phosphorylation at Tyr1045. (**a**–**f**) Fluorescence microscopy of quiescent A431 cells following treatment with EGF or LRIG1 proteins for the designated times. Cells were fixed with 4% paraformaldehyde, permeabilized with 0.25% Triton X-100 and then subjected to immunocytochemistry with an antibody against the EGFR (green). Note the significant internalization of the EGFR evoked by EGF (**b**) with perinuclear (arrows) localization. Nu, nucleus. Scale bars = 5 μm. (**g**–**i**) Fluorescence microscopy of a cell incubated with LRIG1^{ecto} (0.45 μM) for 30 min and stained for EGFR (green) or LRIG1^{ecto} (red). Note the co-localization of the two proteins at the cell surface (arrow). Scale bar = 5 μm. (**j**) Immunoblotting of total A431 cell lysates treated with either EGF (16 nM) or LRIG1^{ecto} (0.45 μM) for the designated times. The immunoblottings were reacted with antibodies against EGFR P-Tyr1045, P-Tyr1068, total EGFR or β-actin as indicated. (**k**) Quantification of EGFR phosphorylation at Tyr1045. The values represent the mean ± s.e.m. of three independent experiments.

Discussion

To prevent the dire consequences of uncontrolled receptor tyrosine kinase activation, a number of controlling mechanisms, both extracellular and intracellular, have been devised during evolution. We report an additional controlling mechanism that leads to the attenuation of receptor signaling without apparent downregulation of the receptor itself. Specifically, we show that the ectodomain of LRIG1, containing only the 15 LRRs, inhibits ligand-dependent and ligand-independent EGFR activation and causes growth inhibition. Even more powerful effects were observed with a chimeric proteoglycan containing the N-terminal portion of decorin – harboring the attachment site for a single chondroitin-dermatan sulfate chain – and the ectodomain of LRIG1. LRIG1^{ecto} was capable of inhibiting growth factor binding, EGFR autophosphorylation and activation of the MAPK signaling cascade in response to EGF. This was confirmed by growth assays, which showed that only cells expressing EGFR were susceptible to the cytostatic effects of soluble LRIG1 ectodomain. In addition, the cytostatic effects appear to be independent of EGFR number, as both A431 and MDA-468 carcinoma cells (which have amplified EGFR) were growth inhibited as equally well as HeLa cells, which express a physiologic number of receptors. Moreover, we provide strong genetic evidence for the requirement of EGFR in LRIG1 biological activity. We employed CHO-K1 cells, which do not constitutively express detectable levels of the EGFR, and found that they did not respond to soluble LRIG1 proteins. However, when cells were genetically engineered to express a functional EGFR-CFP protein, they became responsive to soluble LRIG1 proteins and were growth inhibited by recombinant LRIG1. This is in agreement with the fact that the EGFR-CFP-expressing cells were similarly growth inhibited by EGFR-specific

tyrosine kinase inhibitors, gefitinib (Iressa) (Sordella *et al*., 2004; Pao and Miller, 2005) and the tyrphostin AG1478 (Levitzki and Gazit, 1995). Furthermore, we demonstrate the existence of high-affinity ($K_d = 10$ nM) binding sites on the A431 cells; the vast majority of these (up to 75%) can be competitively displaced by EGF.

Recent evidence indicates that both Kekkon and LRIG proteins have evolved as negative regulators of receptor tyrosine kinase (Carraway and Sweeney, 2001; Gur *et al*., 2004; Laederich *et al*., 2004). However, their modulating activity appears to be distinct: in the case of Kek1, the inhibition of receptor activation is predominant, while in the case of LRIG1, acceleration of receptor ubiquitination and degradation is the principal mechanism of action (Gur *et al*., 2004; Laederich *et al*., 2004; Rubin *et al*., 2005). These data on LRIG1, however, were primarily generated with cells engineered to overexpress LRIG1, and thus, we cannot conclude that such a mechanism of action may be operational *in vivo*, especially when LRIG1 is widely expressed in a variety of normal tissues, but markedly suppressed in several human malignancies (Hedman *et al*., 2002; Thomasson *et al*., 2003).

Shedding of the ectodomain may be an additional mechanism of EGFR control: generation of a soluble ectodomain of LRIG1 via limited proteolysis could attenuate EGFR signaling in a paracrine or autocrine manner. Indeed, a search of two databases for proteases (MEROPS and CUTTER) has revealed numerous potential cleavage sites (including sites cleavable by bone morphogenetic protein-1, proprotein convertase 1 and the peptidase PHEX) within the juxta-membrane region of LRIG1. This processing could liberate the extracellular domain of LRIG1 from the cell surface of malignant cells as well as stromal elements.

In contrast to the transmembranous LRIG1, we did not observe any physical downregulation of the EGFR using the soluble ectodomain. A possible explanation of our findings is that soluble forms of LRIG1 could act at the cell surface by maintaining the EGFR in a monomeric, 'attenuated' or autoinhibited state. The soluble LRIG1 protein could act in a way similar to *cetuximab*, a monoclonal antibody that prevents the unfolding of the EGFR, thereby keeping the receptor in an inactive, tethered configuration, which also prevents the intermolecular interactions that lead to dimerization and activation (Li *et al*., 2005). This interaction not only would attenuate autocrine stimulation of the EGFR mediated by endogenously produced factors such as TGF-α, but would also reduce the stimulation evoked by EGF. This provides a novel mechanistic explanation for the marked growth inhibition in cells expressing EGFR. Utilization of a soluble form of LRIG1 and related gene products could lead to effective treatments of human malignancies in which EGFR plays a primary role. In agreement with this concept, preliminary studies in our laboratory using an orthotopic A431 tumor xenograft model have shown that soluble forms of LRIG1 protein retard *in vivo* tumor growth when systemically administered.

Materials and methods

Cell cultures and reagents

A431, HeLa, MDA-468 and CHO-K1 cells were obtained from American tissue culture collection (Manassas, VA, USA). Dulbecco's modified Eagle's medium (DMEM), fetal bovine serum, 100 × antibiotic–antimycotic solution and Dulbecco's phosphate-buffered saline (DPBS) were purchased from Mediatech (Herndon, VA, USA). All the chemicals, unless specified, were purchased from Sigma (St Louis, MO, USA). Nitrocellulose membrane was purchased from Bio-Rad (Hercules, CA, USA). Recombinant human EGF and anti-Erk1/2 were purchased from Promega (Madison, WI, USA). Antibodies include polyclonal rabbit antibodies against the N-terminal region of decorin (Fisher *et al*., 1995), the C-terminal region of the EGFR (sc-03; Santa Cruz Biotechnology, Santa Cruz, CA, USA), P-Erk1/2 and Tyr1068 and Tyr1045 (Cell Signaling Technology, Beverly, MA, USA), and monoclonal antibodies against β-actin (Sigma, St Louis, MO, USA), phospho-tyrosine (PY20; BD Transduction Laboratories, San Diego, CA, USA), EGFR (Ab-12; NeoMarkers Inc., Union City, CA, USA) and His_6 (CalBiochem, San Diego, CA, USA). Super Signal West Pico chemiluminescent substrate was purchased from Pierce.

Expression and purification of recombinant proteins and rotary shadowing electron microscopy

We cloned the ectodomain of LRIG1 encompassing the 15 LRRs (Ala42 to Leu493), according to the published sequence (National center for biotechnology information (NCBI) ID no. ; AAU44786), into the pCEP-Pu vector containing the BM-40 signal peptide sequence (Kohfeldt *et al*., 1997). The cloned sequence contained 452 amino acids and the expressed protein had a predicted molecular weight of ~53 kDa. To generate Dcn-LRIG1^{ecto}, the first 24 amino acids of the decorin sequence (Met1 to Gly24), containing the glycanation site (Ser7), were cloned between the BM-40 signal peptide and LRIG1^{ecto} sequences. Both constructs contained a His_6 tag at their C-termini. Following complete sequencing, the vectors were stably transfected into human embryonic kidney 293-EBNA cells. Transfectants were selected in media containing G418 (250 μg ml^{-1}) and puromycin (500 ng ml^{-1}) for at least 4 weeks. Isolation and purification of recombinant proteins were as described previously (Mongiat *et al*., 2003; Gonzalez *et al*., 2005). Protein purity was verified by SDS–PAGE and immunoblotting using an anti-His tag antibodies (Goldoni *et al*., 2004). For rotary shadowing, samples were dissolved in 0.1 M ammonium bicarbonate buffer at various dilutions and processed as described before (Keene *et al*., 2000). Images were inspected using Photoshop 7.0 and molecules were measured using the public domain NIH Image program.

Generation of cells expressing EGFR-CFP chimera and growth assays

To determine the specificity of both LRIG1^{ecto} and Dcn-LRIG1^{ecto} recombinant proteins, we transfected CHO-K1 cells, which do not express endogenous EGFR, with a chimeric EGFR-CFP vector (Sorkin *et al*., 2000). Following selection in media containing G418 as above, positive clones were identified by fluorescence microscopy using appropriate filters and by Western immunoblotting with anti-EGFR antibody. Positive clones and wild-type CHO-K1 cells were tested in growth assays in the presence or absence of recombinant proteins as detailed below.

We established a co-culture system where 293-EBNA cells, either wild-type or stably expressing cells, were seeded in the

top trans-well dishes, whereas A431 cells were seeded in the bottom wells. Under such conditions, only soluble factors released from the cells would be able to diffuse through the 0.2-μm membrane separating the two compartments. Cells were grown for 5–6 days without changing the medium and curves were generated by counting the cells. In some cases, we tested media conditioned for 5 days by either wild-type 293 cells or cells secreting either recombinant protein. In these experiments, the media were concentrated fivefold using Centriprep (Millipore Corporation, Bedford, MA, USA). In order to replenish nutrient supplies for target cells, the media were mixed 1:1 (v/v) with 2 × DMEM and 20% serum. Dose–response curves with recombinant LRIG1^{ecto} and Dcn-LRIG1^{ecto} were also performed. Cell number was estimated by either direct counting or by determining OD at 490 nm using the CellTiter 96 (Promega, Madison, WI, USA) assay.

Fluorescence microscopy
Following treatment with either recombinant protein or EGF, cells were fixed with ice-cold 4% paraformaldehyde, permeabilized with 0.25% Triton X-100 for 2 min and subjected to immunofluorescence microscopy using appropriate filters. To detect EGFR, we used either a mouse or rabbit antibody (Ab-12, NeoMarkers and sc-03, Santa Cruz, respectively), followed by fluorescein-isothiocynate (FITC)-conjugated secondary antibody (Santa Cruz). To detect LRIG1^{ecto}, we used a mouse anti-His antibody (Calbiochem), followed by Rhodamine-conjugated secondary antibody. Cells were mounted with Vectashield medium (Vector Laboratories, Burlingame, CA, USA).

Radioligand binding assays
Approximately 20 μg recombinant LRIG1^{ecto} were radiolabeled using ^{125}I and Iodogen beads (Pierce) as described before (Mongiat *et al*., 2003) to reach high-specific activity ($1–8 \times 10^{18}$ c.p.m./mol) and purified via a Sephadex G-50 column. The exclude fractions were analysed by SDS–PAGE and autoradiography, pooled and used in radioligand binding studies using confluent, serum-starved A431 cells at 4°C. Cells were incubated with various concentrations of ^{125}I-labeled LRIG1^{ecto} for 2 h under gentle shaking, washed several times, extracted in radioimmuno-precipitation assay (RIPA) buffer and counted in total. Competition experiments were carried out with 10 and 20 M excess EGF. Overlay assays were carried out essentially as described before (Mongiat *et al*., 2001). Briefly, scalar dilutions of recombinant LRIG1^{ecto} or BSA were slot-blotted into nitrocellulose filters. The filters were air-dried, blocked for 18 h with 5% BSA and incubated for several hours with serum-free media conditioned for 24–48 h by A431 cells. The blots were then washed again and reacted with an anti-EGFR antibody followed by chemiluminenscence detection.

Western blots quantification and statistical analysis
Immunoblots were quantified by scanning densitometry (relative densities) with Scion Image alpha 4.0.3.2 (www.scioncorp.com). For this purpose, blots low in background and showing bands below saturation levels were chosen. Background manipulations were avoided in order not to alter density values. Images were calibrated within the Scion Image program by selecting the lightest (background) and darkest area of the blot. Only curves close to linear were considered to approximate area of pixels. Differences between means were evaluated with an unpaired two-sided Student's *t*-test using the Sigma Plot 9 statistical package. $P<0.05$ was considered as significant.

Abbreviations

EGFR, epidermal growth factor receptor; LRIG1, leucine-rich repeats and immunoglobulin-like domains-1; LRIG1^{ecto}, a soluble form of LRIG1 containing only the extracellular leucine-rich domain; Dcn-LRIG1^{ecto}, a chimeric proteoglycan harboring the N-terminus of decorin fused to LRIG1^{ecto}; CFP, cyan fluorescent protein; SDS–PAGE, sodium dodecylsulfate–polyacrylamide gel electrophoresis.

Acknowledgements

We thank Alexander Sorkin for generously providing the EGFR-CFP construct, Kevin J Williams for the use of the γ-counter, Maurizio Mongiat for supplying the pCEP-Pu vector and Ulrich Rodeck for providing Iressa and valuable suggestions. This work was supported in part by National Institutes of Health Grants RO1 CA39481 and RO1 CA47282, and Department of the Army Grants DAMD17-00-1-0425 (to RVI).

References

Alvarado D, Rice AH, Duffy JB. (2004a). Bipartite inhibition of *Drosophila* epidermal growth factor receptor by the extracellular and transmembrane domains of Kekkon1. *Genetics* **167**: 187–202.

Alvarado D, Rice AH, Duffy JB. (2004b). Knockouts of Kekkon1 define sequence elements essential for *Drosophila* epidermal growth factor receptor inhibition. *Genetics* **166**: 201–211.

Bailly M, Wyckoff J, Bouzahzah B, Hammerman R, Sylvestre V, Cammer M *et al*. (2000). Epidermal growth factor receptor distribution during chemotactic response. *Mol Biol Cell* **11**: 3873–3883.

Batzer AG, Rotin D, Urena JM, Skolnik EY, Schlessinger J. (1994). Hierarchy of binding sites for Grb2 and Shc on the epidermal growth factor receptor. *Mol Cell Biol* **14**: 5192–5201.

Berkers JAM, van Bergen en Henegouwen PMP, Boonstra J. (1991). Three classes of epidermal growth factor receptors on HeLa cells. *J Biol Chem* **266**: 922–927.

Carpenter G. (1987). Receptors for epidermal growth factor and other polypeptide mitogens. *Annu Rev Biochem* **56**: 881–914.

Carpenter G. (2000). The EGF receptor: a nexus for trafficking and signaling. *BioEssays* **22**: 697–707.

Carraway III KL, Sweeney C. (2001). Localization and modulation of ErbB receptor tyrosine kinases. *Curr Opin Cell Biol* **13**: 125–130.

Carter RE, Sorkin A. (1998). Endocytosis of functional epidermal growth factor receptor-green fluorescent protein chimera. *J Biol Chem* **273**: 35000–35007.

Cook PW, Piepkorn M, Clegg CH, Plowman GD, DeMay JM, Brown JR *et al*. (1997). Transgenic expression of the human amphiregulin gene induces a psoriasis-like phenotype. *J Clin Invest* **100**: 2286–2294.

Csordás G, Santra M, Reed CC, Eichstetter I, McQuillan DJ, Gross D *et al*. (2000). Sustained down-regulation of the epidermal growth factor receptor by decorin. A mechanism for controlling tumor growth *in vivo*. *J Biol Chem* **275**: 32879–32887.

Derheimer FA, MacLaren CM, Weasner BP, Alvarado D, Duffy JB. (2004). Conservation of an inhibitor of the epidermal growth factor receptor, Kekkon1, in dipterans. *Genetics* **166**: 213–224.

Ennis BW, Valverius EM, Bates SE, Lippman ME, Bellot F, Kris R *et al*. (1989). Anti-epidermal growth factor receptor antibodies inhibit the autocrine-stimulated growth of MDA-468 human breast cancer cells. *Mol Endocrinol* **3**: 1830–1838.

Filmus J, Pollak MN, Cailleau R, Buick RN. (1985). MDA-468, a human breast cancer cell line with a high number of epidermal growth factor (EGF) receptors, has an amplified EGF receptor gene and is growth inhibited by EGF. *Biochem Biophys Res Comm* **128**: 898–905.

Filmus J, Trent JM, Pollak MN, Buick RN. (1987). Epidermal growth factor receptor gene-amplified MDA-468 breast cancer cell line and its nonamplified variants. *Mol Cell Biol* **7**: 251–257.

Fisher LW, Stubbs III JT, Young MF. (1995). Antisera and cDNA probes to human and certain animal model bone matrix noncollagenous proteins. *Acta Orthop Scand* **66**: 61–65.

Ghiglione C, Amundadottir L, Andresdottir M, Bilder D, Diamonti JA, Noselli S *et al*. (2003). Mechanism of inhibition of the *Drosophila* and mammalian EGF receptors by the transmembrane protein Kekkon 1. *Development* **130**: 4483–4493.

Ghiglione C, Carraway III KL, Amundadottir LT, Boswell RE, Perrimon N, Duffy JB. (1999). The transmembrane molecule kekkon 1 acts in a feedback loop to negatively regulate the activity of the *Drosophila* EGF receptor during oogenesis. *Cell* **96**: 847–856.

Goldoni S, Owens RT, McQuillan DJ, Shriver Z, Sasisekharan R, Birk DE *et al*. (2004). Biologically active decorin is a monomer in solution. *J Biol Chem* **279**: 6606–6612.

Gonzalez EM, Reed CC, Bix G, Fu J, Zhang Y, Gopalakrishnan B *et al*. (2005). BMP-1/Tolloid-like metalloproteases process endorepellin, the angiostatic C-terminal fragment of perlecan. *J Biol Chem* **280**: 7080–7087.

Grovdal LM, Stang E, Sorkin A, Madshus IH. (2004). Direct interaction of Cbl with pTyr 1045 of the EGF receptor (EGFR) is required to sort the EGFR to lysosomes for degradation. *Exp Cell Res* **300**: 388–395.

Guo D, Holmlund C, Henriksson R, Hedman H. (2004). The *LRIG* gene family has three vertebrate paralogs widely expressed in human and mouse tissues and a homolog in Ascidiacea. *Genomics* **84**: 157–165.

Gur G, Rubin C, Katz M, Amit I, Citri A, Nilsson J *et al*. (2004). LRIG1 restricts growth factor signaling by enhancing receptor ubiquitylation and degradation. *EMBO J* **23**: 3270–3281.

Hedman H, Nilsson J, Guo D, Henriksson R. (2002). Is LRIG1 a tumour suppressor gene at chromosome 3p14.3? *Acta Oncol* **41**: 352–354.

Holmlund C, Nilsson J, Guo D, Starefeldt A, Golovleva I, Henriksson R *et al*. (2004). Characterization and tissue-specific expression of human LRIG2. *Gene* **332**: 35–43.

Iozzo RV. (1997). The family of the small leucine-rich proteoglycans: key regulators of matrix assembly and cellular growth. *Crit Rev Biochem Mol Biol* **32**: 141–174.

Iozzo RV. (1998). Matrix proteoglycans: from molecular design to cellular function. *Annu Rev Biochem* **67**: 609–652.

Iozzo RV. (1999). The biology of the small leucine-rich proteoglycans. Functional network of interactive proteins. *J Biol Chem* **274**: 18843–18846.

Iozzo RV, Moscatello D, McQuillan DJ, Eichstetter I. (1999). Decorin is a biological ligand for the epidermal growth factor receptor. *J Biol Chem* **274**: 4489–4492.

Iozzo RV, Murdoch AD. (1996). Proteoglycans of the extracellular environment: clues from the gene and protein side offer novel perspectives in molecular diversity and function. *FASEB J* **10**: 598–614.

Jiang X, Huang F, Marusyk A, Sorkin A. (2003). Grb2 regulates internalization of EGF receptors through clathrin-coated pits. *Mol Biol Cell* **14**: 858–870.

Jiang X, Sorkin A. (2002). Coordinated traffic of Grb2 and Ras during epidermal growth factor receptor endocytosis visualized in living cells. *Mol Biol Cell* **13**: 1522–1535.

Keene DR, San Antonio JD, Mayne R, McQuillan DJ, Sarris G, Santoro SA *et al*. (2000). Decorin binds near the C terminus of type I collagen. *J Biol Chem* **275**: 21801–21804.

Kohfeldt E, Maurer P, Vannahme C, Timpl R. (1997). Properties of the extracellular calcium binding module of the proteoglycan testican. *FEBS Lett* **414**: 557–561.

Laederich MB, Funes-Duran M, Yen L, Ingalla E, Wu X, Carraway III KL *et al*. (2004). The leucine-rich repeat protein LRIG1 is a negative regulator of ErbB family receptor tyrosine kinases. *J Biol Chem* **279**: 47050–47056.

Levitzki A, Gazit A. (1995). Tyrosine kinase inhibition: an approach to drug development. *Science* **267**: 1782–1788.

Levkowitz G, Waterman H, Ettenberg SA, Katz M, Tsygankov AY, Alroy I *et al*. (1999). Ubiquitin ligase activity and tyrosine phosphorylation underlie suppression of growth factor signaling by c-Cbl/Sli-1. *Mol Cell* **4**: 1029–1040.

Li S, Schmitz KR, Jeffrey PD, Wiltzius JJ, Kussie P, Ferguson KM. (2005). Structural basis for inhibition of the epidermal growth factor receptor by cetuximab. *Cancer Cell* **7**: 301–311.

Moghal N, Sternberg PW. (1999). Multiple positive and negative regulators of signaling by the EGF-receptor. *Curr Opin Cell Biol* **11**: 190–196.

Mongiat M, Otto J, Oldershaw R, Ferrer F, Sato JD, Iozzo RV. (2001). Fibroblast growth factor-binding protein is a novel partner for perlecan protein core. *J Biol Chem* **276**: 10263–10271.

Mongiat M, Sweeney S, San Antonio JD, Fu J, Iozzo RV. (2003). Endorepellin, a novel inhibitor of angiogenesis derived from the C terminus of perlecan. *J Biol Chem* **278**: 4238–4249.

Musacchio M, Perrimon N. (1996). The *Drosophila kekkon* genes: novel members of both the leucine-rich repeat and immunoglobulin superfamilies expressed in the CNS. *Dev Biol* **178**: 63–76.

Nilsson J, Starefeldt A, Henriksson R, Hedman H. (2003). LRIG1 protein in human cells and tissues. *Cell Tissue Res* **312**: 65–71.

Nilsson J, Vallbo C, Guo D, Golovleva I, Hallberg B, Henriksson R *et al*. (2001). Cloning, characterization, and expression of human LIG1. *Biochem Biophys Res Comm* **284**: 1155–1161.

Okutani T, Okabayashi Y, Kido Y, Sugimoto Y, Sakaguchi K, Matuoka K *et al*. (1994). Grb2/Ash binds directly to tyrosines 1068 and 1086 and indirectly to tyrosine 1148 of activated human epidermal growth factor receptors in intact cells. *J Biol Chem* **269**: 31310–31314.

Pao W, Miller VA. (2005). Epidermal growth factor receptor mutations, small-molecule kinase inhibitors, and non-small-cell lung cancer: current knowledge and future directions. *J Clin Oncol* **23**: 2556–2568.

Reed CC, Gauldie J, Iozzo RV. (2002). Suppression of tumorigenicity by adenovirus-mediated gene transfer of decorin. *Oncogene* **21**: 3688–3695.

Reed CC, Waterhouse A, Kirby S, Kay P, Owens RA, McQuillan DJ *et al*. (2005). Decorin prevents metastatic spreading of breast cancer. *Oncogene* **24**: 1104–1110.

Rubin C, Gur G, Yarden Y. (2005). Negative regulation of receptor tyrosine kinases: unexpected links to c-Cbl and receptor ubiquitylation. *Cell Res* **15**: 66–71.

Santra M, Reed CC, Iozzo RV. (2002). Decorin binds to a narrow region of the epidermal growth factor (EGF) receptor, partially overlapping with but distinct from the EGF-binding epitope. *J Biol Chem* **277**: 35671–35681.

Schlessinger J. (2003). Signal transduction. Autoinhibition control. *Science* **300**: 750–752.

Sigismund S, Woelk T, Puri C, Maspero E, Tacchetti C, Transidico P *et al*. (2005). Clathrin-independent endocytosis of ubiquitinated cargos. *Proc Natl Acad Sci USA* **102**: 2760–2765.

Sordella R, Bell DW, Haber DA, Settleman J. (2004). Gefitinib-sensitizing *EGFR* mutations in lung cancer activate anti-apoptotic pathways. *Science* **305**: 1163–1167.

Sorkin A, McClure M, Huang F, Carter R. (2000). Interaction of EGF receptor and Grb2 in living cells visualized by fluorescence resonance energy transfer (FRET) microscopy. *Curr Biol* **10**: 1395–1398.

Suzuki Y, Miura H, Tanemura A, Kobayashi K, Kondoh G, Sano S *et al*. (2002). Targeted disruption of LIG-1 gene results in psoriasiform epidermal hyperplasia. *FEBS Lett* **521**: 67–71.

Suzuki Y, Sato N, Tohyama M, Wanaka A, Takagi T. (1996). cDNA cloning of a novel membrane glycoprotein that is expressed specifically in glial cells in the mouse brain. *J Biol Chem* **271**: 22522–22527.

Thomasson M, Hedman H, Guo D, Ljungberg B, Henriksson R. (2003). LRIGI and epidermal growth factor receptor in renal cell carcinoma: a quantitative RT–PCR and immunohistochemical analysis. *Br J Cancer* **89**: 1285–1289.

Vassar R, Fuchs E. (1991). Transgenic mice provide new insights into the role of TGF-alpha during epidermal development and differentation. *Genes Dev* **5**: 714.

Waterman H, Katz M, Rubin C, Shtiegman K, Lavi S, Elson A *et al*. (2002). A mutant EGF-receptor defective in ubiquitylation and endocytosis unveils a role for Grb2 in negative signaling. *EMBO J* **21**: 303–313.

Weber W, Gill GN, Spiess J. (1984). Production of an epidermal growth factor receptor-related protein. *Science* **224**: 294–297.

Yarden Y, Harari I, Schlessinger J. (1985). Purification of an active EGF receptor kinase with monoclonal antireceptor antibodies. *J Biol Chem* **260**: 315–319.

Zhu J-X, Goldoni S, Bix G, Owens RA, McQuillan D, Reed CC *et al*. (2005). Decorin evokes protracted internalization and degradation of the EGF receptor via caveolar endocytosis. *J Biol Chem* **280**: 32468–32479.